

Evaporation cools the surrounding air because the process requires energy, which is absorbed from the environment as heat, thereby lowering the temperature of the surroundings.

ARTICLE

<https://doi.org/10.1038/s43247-023-00897-0>

OPEN

daily, of each day

Wet bulb temperature is the lowest temperature to which air can be cooled by the evaporation of water into the air at a constant pressure. It is therefore measured by wrapping a wet wick around the bulb of a thermometer and the measured temperature corresponds to the wet bulb temperature.

The diurnal variation of wet bulb temperatures and exceedance of physiological thresholds relevant to human health in South Asia

relating to the branch of biology that deals with the normal functions of living organisms and their parts

Jenix Justine¹, Joy Merwin Monteiro^{2,3✉}, Hardik Shah² & Neethi Rao⁴

Extreme heat is increasingly being acknowledged as a serious hazard to human health, through a combination of physiological responses to heat, expressed as dry and wet bulb temperatures, and personal factors. Here we present an analysis of the diurnal variability of dry and wet bulb temperatures using station data in South Asia during both regular and heatwave days. We find that diurnal cycles differ, with the daily maximum wet bulb temperature occurring several hours after the daily maximum dry bulb temperature. Using radiosonde profiles, we show that the timing and amplitude of the diurnal variability of wet bulb temperature can be explained by changes in boundary layer depths and water content. Physiological thresholds for uncompensable heat stress were exceeded even in the evenings, many hours after dry bulb temperature peaks. Cumulative exceedances occurred in 105 instances, corresponding to at least 300 hours of exposure to uncompensable heat stress in South Asia between 1995 and 2020. We conclude that physiologically relevant thresholds provide a more robust way to estimate health impacts, and that wet bulb temperature alone is insufficient as an indicator of hazardous heat.

Radiosonde profiles are vertical measurements of atmospheric parameters like pressure, temperature, and humidity taken by a radiosonde, a small instrument package carried aloft by a weather balloon, providing valuable data for weather forecasting and climate studies.

In the context of fluid dynamics, "boundary layer depth" or "boundary layer thickness" refers to the distance from a surface where the fluid's velocity changes significantly due to friction and viscous forces, approaching the free-stream velocity.

"Cumulative exceedance" refers to the probability that a specific value or event will be exceeded, considering all previous instances of that value or event, and is often used in risk management and statistical analysis.

Heat stress occurs when the body's core temperature rises to dangerous levels, unable to cool itself through sweating, potentially leading to heat-related illnesses like exhaustion, heat rash, and heatstroke. Heat rash, also known as prickly heat or miliaria, is a skin irritation caused by sweat ducts becoming blocked or inflamed, resulting in small, itchy bumps or blisters.

Extreme heat poses significant health risks, leading to conditions like heat exhaustion and stroke, exacerbating existing illnesses, and increasing the risk of cardiovascular and respiratory problems

¹ College of Climate Change and Environmental Science, Kerala Agricultural University, Vellanikkara, India. ² Department of Earth and Climate Science, Indian Institute of Science Education and Research Pune, Pune, India. ³ Department of Data Science, Indian Institute of Science Education and Research Pune, Pune, India. ⁴ Institute of Public Health, Bengaluru, India. ✉email: joy@iiserpune.ac.in

Extreme heat is increasingly being acknowledged as a serious hazard to human health^{1–3}. The health impacts of exposure to extreme heat occurs due to a combination of physiological responses to heat and other factors such as age, comorbidities and behavioural traits, making it difficult to quantify the impacts of extreme heat⁴. Furthermore, human thermal environments are determined by the ambient temperature, humidity, shortwave/longwave radiation and wind speed, not all of which are routinely and widely measured. These challenges in quantifying both heat exposure and heat stress have resulted in the development of a wide variety of metrics, some of which are simply indicators of the ambient environment whereas others are more physiologically based^{5–12}. Temperature and humidity have been widely and reliably measured over many decades all around the globe, and since direct heat transfer and evaporation of sweat are both pathways for removal of heat from the human body, metrics that incorporate both ambient temperature and humidity have come to be widely used to quantify heat stress.

Since sweating and resulting evaporation from the skin are the primary mechanism for loss of heat from the body, heat stress due to environmental conditions can be categorised as compensable or uncompensable depending on whether the evaporative cooling required to compensate heat gain by the body is lesser or greater than the maximum evaporative cooling that can be provided by the production and evaporation of sweat¹³. For instance, at a given temperature, higher levels of humidity make evaporative cooling less efficient and reduce the body's ability to lose heat; therefore hot, humid environments are more likely lead to uncompensable heat stress. It is such considerations that led to the suggestion that an ambient wet-bulb temperature of 35 °C represents the limit of human physiological adaptation, since it is no longer possible to compensate for heat gain by evaporation of sweat¹⁴.

Both in current and projected future climates, South Asia stands out as one of the hotspots of extreme heat^{15–17}. Furthermore, South Asia is home to a large population that is vulnerable to increases in extreme heat¹⁸. The Indian Meteorological Department's heat wave definition and thresholds were primarily based on dry-bulb temperature (TD)¹⁹, although recent bulletins also provide relative humidity and wind speed. On the basis of TD, two regions of heat wave activity are generally recognised – one in the northwest part of the India and the adjoining Indus river basin, and the east coast of India^{19,20}. More recent studies use wet-bulb temperatures (TW) as a measure of heat stress and delineate regions that experience extreme TW in current and future climates^{15,21}.

While there have been multiple studies of extreme TW recently^{15,17,21,22}, studies are also needed to examine periods of extreme TD since (as we will show in subsequent sections)

- Nearly every heatwave with recorded mortality has occurred in months with high values of extreme TD rather than extreme TW.
- Most high impact heat waves in South Asia in recent years were marked by extreme TD rather than TW.

Therefore, while extreme TW might be a concern in the coming decades, understanding meteorological conditions characterised by extreme TD is very relevant in the current (and likely in the future) climate. Furthermore, recent thermal physiology experiments²³ demonstrate that uncompensable heat stress is achieved at much lower TW than the 35 °C adaptation limit¹⁴, and that this threshold decreases with increasing TD. From a meteorological perspective, the above experiments imply that understanding the relationship between the diurnal cycles of TW and TD might suggest what times of the day are likely to be more hazardous in terms of health impacts.

Few studies exist which actually look at health impacts of extreme heat in South Asia, primarily due to a lack of high quality health data^{24–28}. Given this lack, using physiological data to contextualise TD and TW variability in South Asia provides an alternative methodology to identify regions and periods that are hazardous to human health. Furthermore, these studies represent each day using a single value of TD (maximum, minimum or mean)²⁷. While this choice is made since the response variable (usually all-cause mortality) is also at daily resolution, ignoring the relationship between the diurnal variability of TD and TW makes it difficult to quantify the actual duration for which hazardous environmental conditions exist during each day.

In this study, we document the seasonal variability of extreme TD and TW to contextualise subsequent statistical analyses. We document the timing of daily maximum and minimum of TD and TW and how this timing changes during heat waves. We then use radiosonde data to understand change in timing and amplitude in terms of boundary layer heights and water content. To understand the likely implications on human health, we contextualise TD and TW variability using recent thermal physiological experiments which establish TD/TW combinations that correspond to uncompensable heat stress.

Results and discussion

Monthly variability of mean and extreme TD/TW in South Asia. Most documented heatwaves in South Asia have occurred between the months of March–June (see Supplementary table S1 and the EM-DAT data). In fact, The top ten heatwaves in terms of mortality in the EM-DAT database have predominantly occurred in the months of May and June.

The distribution of mean and extreme TD and TW during the months of March–August for South Asia is presented in Fig. 1. This distribution shows that extreme TD peaks in May whereas extreme TW peaks in July. Extreme TD drops dramatically in July and August whereas extreme TW remains consistently high between June and August. This distribution is consistent with the timing of the onset of the monsoon over South Asia – The monsoon onset over South India is usually in the first week of June and covers most of South Asia by mid-July²⁹. The high precipitation and cloudiness associated with the monsoon would increase near-surface humidity (thus increasing TW) but reduce near-surface TD. This seasonal behaviour is not sensitive to the choice of percentile used to define extreme TD and TW. A similar seasonal cycle is observed in the net solar radiation, with maximum insolation in May (see supplementary fig. S1).

This seasonal distribution of TD and TW also supports the fact that extreme TW alone is insufficient to explain the seasonal distribution of health impacts – May exhibits lower values of extreme TW as compared to June–August but has the highest number recorded mortality due to heat waves. Furthermore, this observation is also consistent with experimental work that suggests that uncompensable heat stress occurs for relatively lower values of TW for high values of TD²³.

While the monthly distribution of extreme TD and TW may suggest a diminished role for extreme TW, this may not be true for individual high-impact heatwaves. For instance, in the analysis of the high impact heatwave in Karachi in June 2015, it was suggested that elevated temperature and humidity were responsible for the unprecedented mortality on the basis of the observed heat index³⁰. However, station data for that period (supplementary figs. S3 and S4) shows that there was a considerable drop in daily minimum humidity (and TW) during the event, and the daily maximum values of humidity and TW were otherwise close to their seasonal mean values.

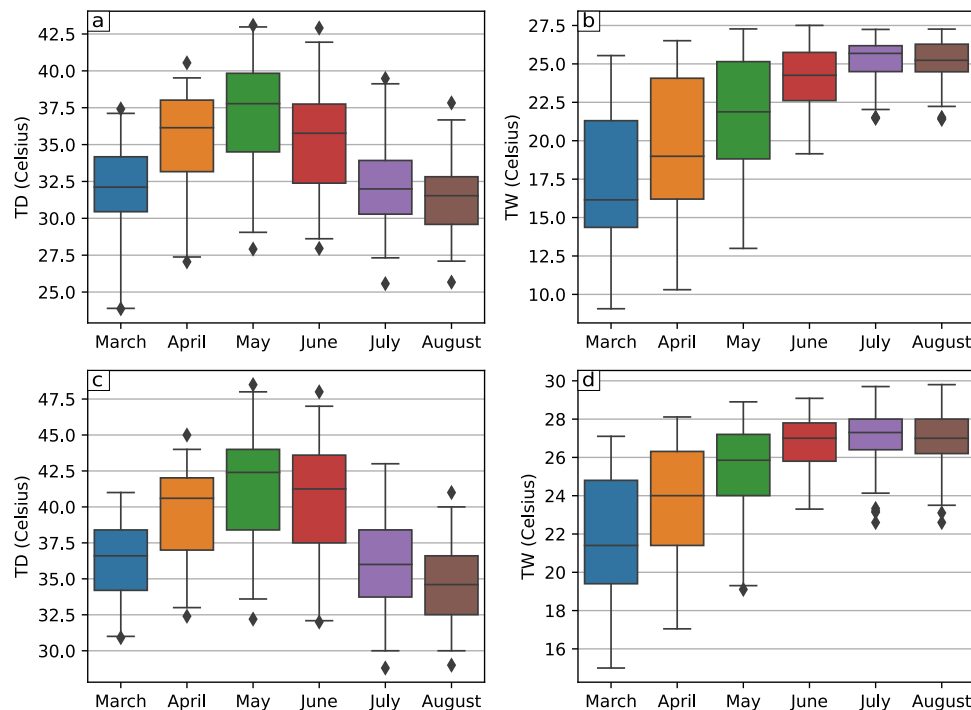


Fig. 1 Seasonal distribution of TD and TW in South Asia. The monthly distribution of the mean (panels **a, b**) and 95th percentile (panels **c, d**) of TD and TW for all stations in South Asia. The whiskers represent the 1st and 99th percentile of each distribution.

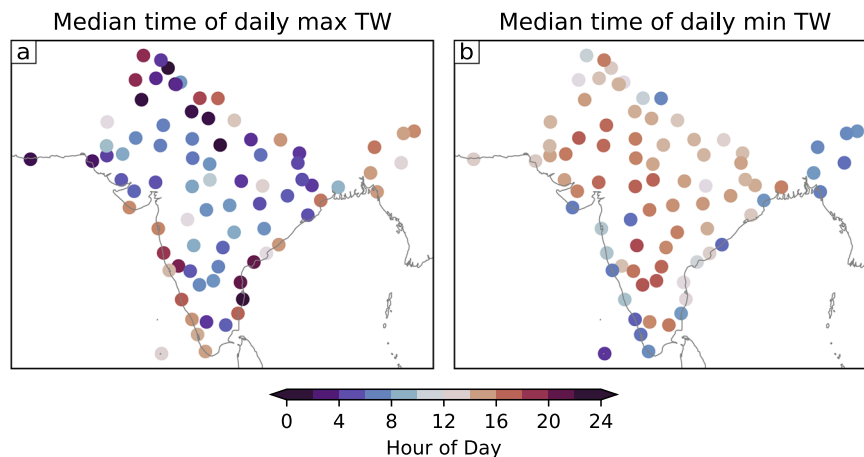


Fig. 2 Timing of TW daily maximum and minimum. The mean hour in local time at which daily maximum (**a**) and minimum (**b**) TW is reached in South Asian stations. The lighter colours represent hours close to noon (hot times of the day) whereas the darker colours represent cooler times of the day.

Analysis of station data from coastal Andhra Pradesh (supplementary figs. S5 and S6) also shows that high impact events in this region were also characterised by **elevated TD rather than elevated TW**. Extreme TW exceeding 30 °C (and for very brief periods exceeding 35 °C) have been observed in some parts of South Asia^{17,21}, but they do not seem to occur during years of high documented mortality. Heat related morbidity is poorly documented in South Asia, and we were able to find only one such study³¹; It may be possible that extreme TW experienced in South Asia contributes to the morbidity rather than mortality burden.

As discussed in this section, high impact heatwaves appear to be associated with **very high daily maximum TD, unchanged daily maximum TW and a drop in daily minimum TW**. While the changes in the diurnal cycle of TD during heatwaves have been analysed previously^{32,33}, a similar analysis for TW, and its relationship with TD have not been documented. In the

subsequent sections, we document and attempt to explain two features – the timing and amplitude – of the diurnal cycle of TW in South Asia.

Timing of the diurnal cycle of TW. The timing of daily maximum and minimum TW is presented in Fig. 2. The majority of stations in South Asia exhibit the same pattern – **the daily maximum TW occurs early in the morning or late in the evening whereas the daily minimum occurs closer to noon**. Regions that are a noticeable exception to this pattern are a cluster of stations in the north-east of India and along the west coast of India. This pattern persists during heatwaves as well, with **the timing of daily maximum TW getting further concentrated into the cooler times of day and vice versa** (see supplementary fig. S7). This phasing can be explained by looking at boundary layer (BL) heights and water vapour content. **In coastal stations, BL water vapour**

content is nearly constant through the day whereas BL heights are highest during the warmest times of the day and become shallow as the land surface cools down. Thus, the ratio of BL water vapour to height increases during the cooler times of the day (see supplementary fig. S11). Assuming a well-mixed boundary layer, this relationship between BL height and water vapour implies that near-surface humidity (and therefore TW) is highest during the cooler times of the day. A similar analysis in stations away from the coast shows that though BL water vapour and height both increase during the day, the ratio of BL water vapour to height reduces due to a larger relative change in BL heights as compared to water vapour (see supplementary fig. S12. While data from only two stations are presented in the supplementary material, we have analysed data from all stations across South Asia which have sufficient observations.). As a result, again the highest TW is experienced in the coolest times of the day. Note that TW is relatively insensitive to changes in TD²¹, and therefore changes in TW closely mirror changes in specific humidity.

Given the experimental evidence for the dependence of critical TW on TD in the context of uncompensable heat stress²³, the significance of extremely high TW (which occurs in the coolest times of the day) in the context of human health is unclear; we will return to this issue in the subsequent section.

Amplitude of the diurnal cycle of TW. The change in amplitude of the diurnal cycle can occur either due to an increase in the daily maximum TW or reduction in the daily minimum TW or both. Figure 3 shows the relationship between the monthly mean and standard deviation of daily maximum and minimum TW for all stations in South Asia. Both quantities show an inverse relationship to the mean value, with stations that are more humid on average exhibiting lower variability in TW. This inverse relationship implies that stations with a higher mean humidity (such as those on the coasts) have smaller variability in the amplitude of the diurnal cycle of TW.

The daily minimum TW shows consistently higher variability across all bins as compared to the daily maximum. The lower variability of daily maximum TW suggests energetic and/or water availability constraints might cap this variability, though a detailed analysis is out of the scope of this work. For the stations with the highest mean TW (which are more likely to experience harmful values of TW), the low variability of daily maximum TW implies that even extreme values of TW are in fact very close to the median value. In summary, Fig. 3 shows that on average, the amplitude of TW diurnal variability reduces with increasing mean TW, and that amplitude of the diurnal cycle of TW is mainly controlled by the daily minimum TW as the mean TW increases.

Changes to the diurnal cycle of TW during heatwaves. While the previous figure shows that daily maximum TW is more tightly distributed about the mean as compared to the daily minimum, it is unclear if this relationship holds true during heatwaves (i.e. in the tail of the distribution).

Figure 4 presents the change in the diurnal range of TW during extreme days as compared to the change in daily maximum and minimum TW. Remarkably, the majority of stations exhibit very little change in the daily maximum TW, and the diurnal range is almost entirely accounted for by changes in daily minimum TW, which as we have seen occurs during the hottest times of the day. In contrast with the overall picture presented in Fig. 3, the amplification of the diurnal cycle of TW during heatwaves does not exhibit any clear relationship with the mean TW.

A first order explanation of the observed changes in the diurnal range during heatwave days can be obtained by examining the changes in BL properties. The distribution of BL heights and water vapour content during regular and extreme days presented in Fig. 5 suggests that a strong amplification of the diurnal cycle of TW occurs in stations whose BL water vapour content shows a smaller increase (0.16σ , $p < 0.02$ in a two sample t-test) relative to the increase BL heights (0.57σ , $p < 10^{-5}$ in a two sample t-test) during heatwaves. Therefore, the same amount of water vapour is mixed through a greater height, resulting in a reduction of near-surface TW, which is very sensitive to changes in water vapour. Conversely, stations which show a smaller amplification of the diurnal cycle have a smaller increase in BL heights and larger increase in water vapour content during heat waves (0.48σ and 0.59σ for BL height and water vapour respectively, see supplementary fig. S13). This contrast in behaviour suggests that the diurnal cycle of TW is strongly amplified in locations where the additional energy added to the atmosphere during heatwaves is unable to elicit a corresponding response in terms of latent heat fluxes, which is also dependent on land surface properties³⁴. Alternatively, boundary layer water vapour could controlled by other factors such as land-sea breezes.

Timing of critical TW exceedances and public health implications. The hour of day when critical TW thresholds are exceeded are presented in Fig. 6. Of the few instances when the absolute thresholds were exceeded, and the highest number of these occur in the evening at 6 p.m., close to sunset. This is a direct result of the phase difference between the diurnal cycles of TD and TW: TW rapidly rises from its daily minimum value around noon, and there is a time when falling TD and rising TW coincide to exceed critical TW thresholds. As the threshold is reduced (to account for increased susceptibility to heat stress in certain individuals, see “Discussion” in subsection 4.5), the hour

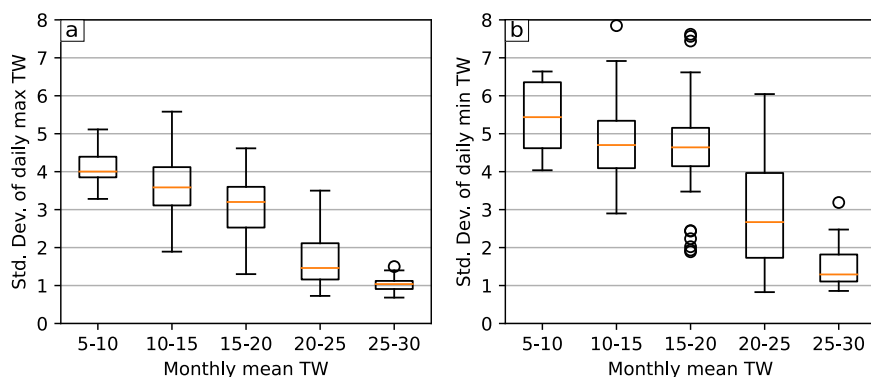


Fig. 3 Relationship between mean and variance of TW. The relationship between monthly mean TW and the respective standard deviation for daily maximum (a) and minimum TW (b) for all stations in South Asia. The calculation was done for the months March to June, and each month was treated separately. Thus, each station contributes four values. The monthly mean bins are in degrees centigrade.

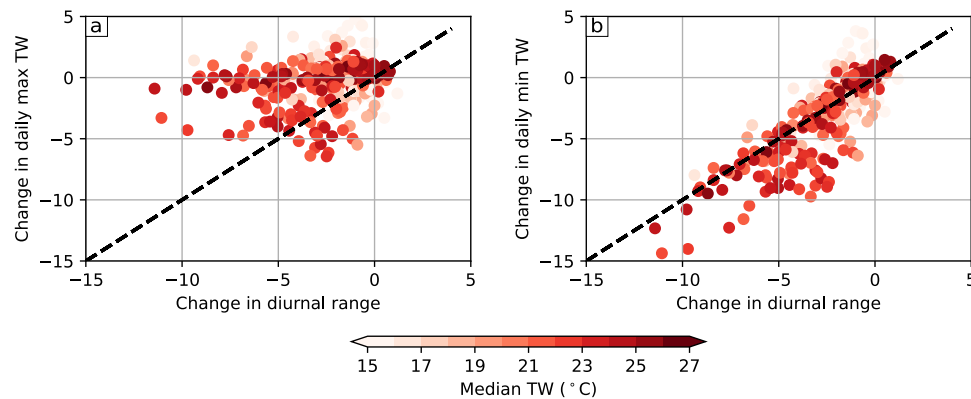


Fig. 4 Change in TW diurnal range during heatwaves. The change in median daily maximum (a) and minimum (b) TW between regular and extreme days. The diurnal range is defined as the difference between the median daily maximum and daily minimum TW. The shading of each point corresponds to the monthly median TW, with darker shades representing higher TW.

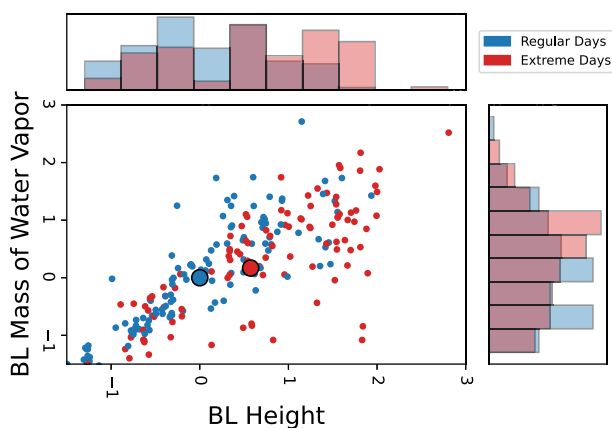


Fig. 5 Change in boundary layer properties during heatwaves. The distribution of boundary layer heights and water vapour content during regular (blue) and extreme (red) days in stations that exhibit an amplification of the diurnal cycle of TW during extreme days. Both quantities are normalised by the mean and standard deviation of the distribution during regular days. Thus, the axes are in units of standard deviation of regular days. The large blue and red dots denote the mean during regular and extreme days respectively.

of maximum exceedance shifts to 3 p.m. (close to the warmest time of the day), but the sum of the noon (12 p.m.) and evening (6 p.m.) exceedances are still larger than those during 2 p.m. It is important to note here that **threshold exceedances rarely, if ever occur during the time of daily maximum TW**. This is because while TW continues to increase into the night, TD decreases and the combination of TD and TW no longer exceed the critical thresholds. Therefore, our results suggest that health-oriented analyses may benefit from focusing on physiological threshold exceedances which are a combination of TD and TW, and likely to contribute more to mortality than extreme TD or TW alone. We reiterate that these thresholds are mainly used as indicators in our study, and more research is required to identify thresholds for South Asian populations.

Spatial pattern of TD/TW exceedances. The spatial pattern of TW exceedances for the entire time period (1995–2020) is presented in Fig. 7. Most of the absolute exceedances occur in **Pakistan's Sindh region, a region known for extreme TW and TD²¹**. Reducing the critical TW thresholds suggests that stations close to critical TW threshold exceedance are concentrated along

the east coast of India and the Indus river basin in Pakistan. The spatial pattern of 80% critical TW exceedance is useful to identify regional hotspots: east coast of India (not the west coast, though it has similar values of mean and extreme TW, see supplementary fig. S8) during May and the Indus and Gangetic plains in Pakistan and India respectively during June. This shift in the pattern northwards likely reflects the seasonality of the monsoon onset, which occurs over north India and Pakistan only by the end of June resulting in higher humidity and temperatures in these regions in June rather than May (see supplementary fig. S8). These exceedances also correspond well with the fact that high impact heatwaves usually occur in May along the east coast of India and in June in north India and Pakistan (see EM-DAT data in supplementary material). Central India and northwestern parts of India don't experience many instances of TW exceedance, even though they experience some of the most extreme TD in the region (see supplementary fig. S8). Exceedances during individual high impact heatwaves in South Asia are also high in regions that have experienced high mortality (see supplementary fig. S9), though there are variations which are likely due to non-climatic factors such as differences in reporting, preparedness, population vulnerability.

Conclusion

The impacts of extreme heat on human health are beginning to be well understood, and the mechanisms through which heat affects human health are recognised^{4,35}. In this work, we integrate experimental studies of the impact of heat on human physiology with the analysis of the diurnal cycle of TW to complement existing epidemiological studies on heat and health.

We show that the timing and amplitude of the diurnal cycle of TW are quite different from that of TD. While a detailed analysis of the mechanisms governing these features is beyond the scope of this work, we show that relative changes in BL heights and water vapour content provide a first order explanation for the observed phase and amplitude of the TW diurnal cycle. Our analysis suggests that the phase difference between TD and TW is important in the occurrence of critical TW threshold crossings, especially during heatwaves; any shift in phase from the nearly anticorrelated diurnal cycles of TD and TW will result in an increase of instances when critical TW thresholds are exceeded. Thus, the physical mechanisms governing the TW diurnal cycle are as important to understand as the mechanisms governing the occurrence of extreme TW^{36–38}.

Since the initial work exploring the relationship between TW and limits to human adaptation¹⁴, there has been renewed interest in studying TW within the climate science community,

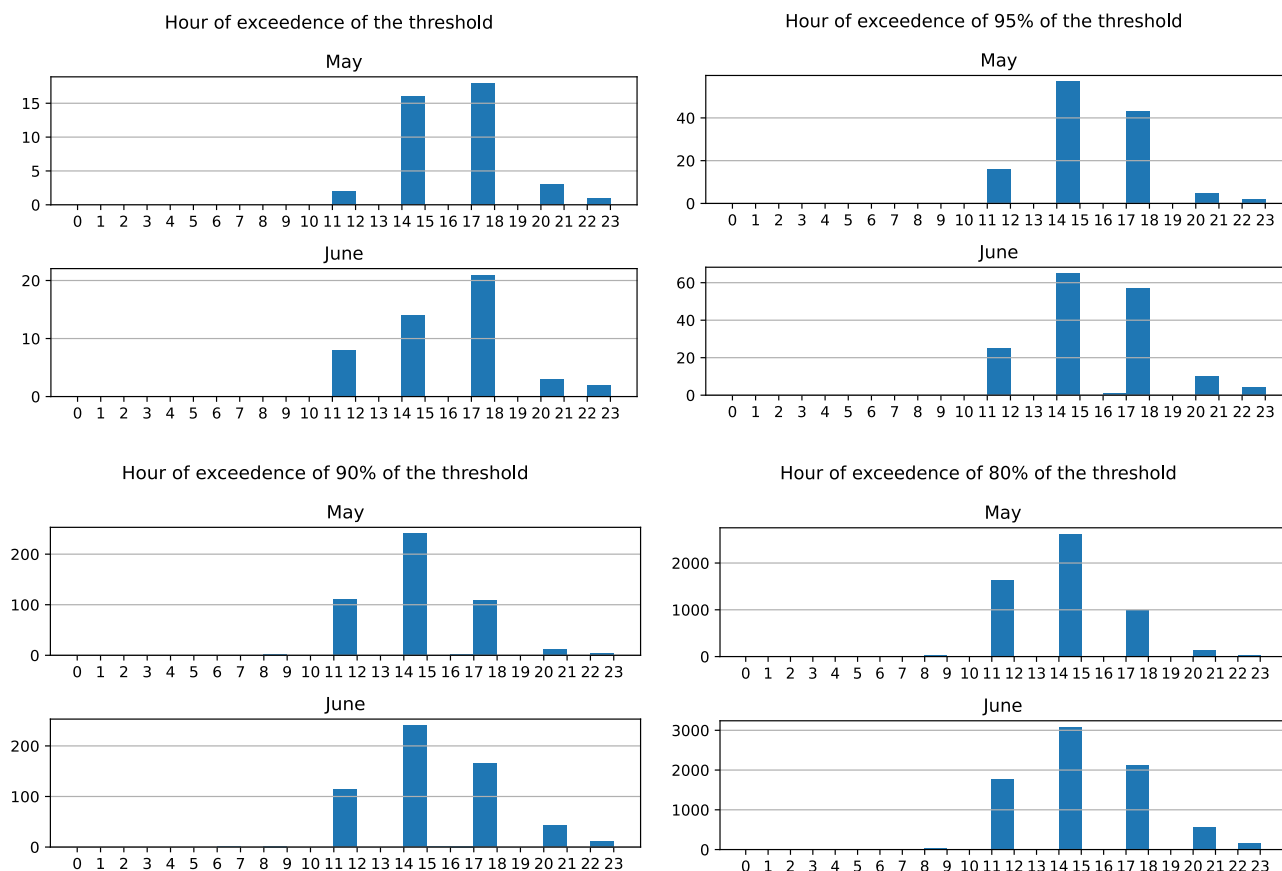


Fig. 6 Timing of exceedance of physiological thresholds. The number of instances of critical TW exceedances over the day. The x-axis represents hour of day in local time. Only the results from May and June are presented since they exhibit the largest number of exceedances in South Asia.

and multiple studies following it have explored mechanisms and processes leading to extreme TW globally^{15,17,21,22,30,38}. The regions of extreme TW that were identified in these studies within South Asia are quite similar to those identified in our own analysis. While these regions are indeed characterised by high climatological TW, they are not characterised by elevated TW when high-impact heatwaves occurred (i.e., >1000 deaths). In these instances, we observe a reduction in daily minimum TW, leading to a daily mean TW value that is actually lower than the average. In the hot, dry conditions experienced during high-impact heatwaves, evaporative cooling is limited by physiological mechanisms such as the ability to produce sweat¹³. Therefore, dehydration and improper thermoregulation can lead to uncompensable heat stress even if TW is low. On the other hand, when ambient TW is high, evaporative cooling is limited by the atmosphere's ability to accept additional water vapour. In such conditions, extreme TW can likely be a reliable indicator of health impacts. While concern is rising regarding the health impacts of extreme TW (the recent IPCC report specifically mentions TW and South Asia³⁹), most epidemiological studies in South Asia²⁷ use TD as a predictor and find significant association between TD and mortality. Our results show how the relationship of the diurnal cycles of TD and TW in South Asia and experimentally derived physiological thresholds help reconcile these seemingly contradictory viewpoints⁴⁰. Furthermore, by focusing on physiological thresholds rather than meteorological indicators, we were able to find that hazardous conditions can occur at times much removed from the time of either daily max TD or TW¹².

Our results suggest that caution must be exercised while using reanalysis and climate model outputs to understand heat stress in current and future climates. Projections based on daily or

monthly mean values must be appropriately qualified since they average over the diurnal cycle. For example, if we compute instances of absolute threshold exceedance using daily mean TD and TW for the current dataset, we observe exceedance on only three days as compared to eighty days when we use sub-daily data. Furthermore, it must be verified whether reanalysis products can capture the amplitude of the diurnal cycle of TW adequately, especially during heatwaves. If the amplification of the diurnal cycle is muted, this could mean that the modelled daily minimum value of TW is higher than observations, and the likelihood of exceedance will correspondingly increase.

The spatial distribution of critical TW exceedance shows clear hotspots, and it is worth noting that this spatial distribution of exceedance of physiological thresholds matches well with the state-wise distribution of mortality reported in India (see supplementary fig. S9). Given the paucity of high quality, long term health data in South Asia which is essential for epidemiological analyses, studies to identify appropriate critical physiological thresholds for South Asian populations combined with high resolution station data could provide important insight into the burden of heat stress in South Asia and help identify hotspots. Therefore, we suggest that it is important to improve the spatial and temporal resolution of meteorological observations to help identify potential hotspots for enhanced public health monitoring.

The timing of critical TW exceedance has implications for public health communication during heatwaves which usually advise against physical activity during the hours of peak heat, which are usually in the afternoons⁴¹. The fact that critical TW exceedance is also observed later in the evening (and sometimes at night) must also be reflected in public health messaging. Heat

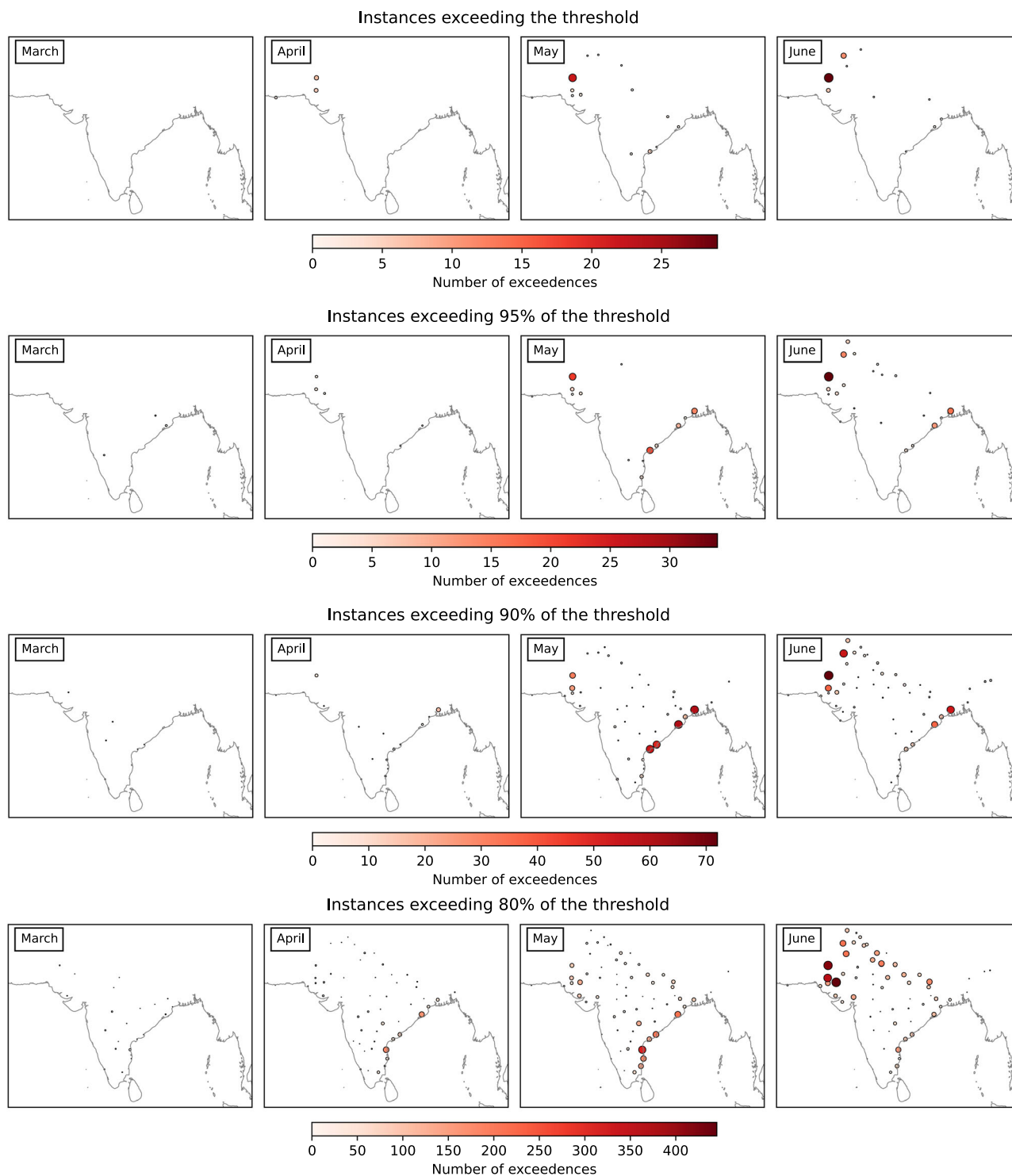


Fig. 7 Spatial distribution of frequency of exceedance of physiological thresholds. The spatial patterns of threshold TW exceedance in South Asia for different months. Both the colour of the dots as well as their size indicate the magnitude of number of exceedances at each station.

adaptation policies have to become more holistic, considering activity and exposure over the whole day rather than focusing on certain hours of the day. Such policies could take into account location (e.g., workplace, school or home), timing and duration of exposure to uncompensable heat stress while devising appropriate public health strategies.

A key limitation of our analysis is that the physiological thresholds were determined using subjects who are unlikely to be representative of the South Asian population. Nevertheless, we

believe that the analysis still is informative and instructive and points to the need for such thermal physiology studies in South Asia. We use station data since it represents actual measurements rather than model-derived data; However, this limited our analysis to three-hourly resolution which might underestimate the actual exposure to hazardous levels of heat. Furthermore, since station data is present only at a few locations all over South Asia, we could only present broad regional patterns and could have missed locations with potentially higher exposure to hazardous

levels of heat. Gridded datasets, after careful verification of the diurnal cycles of TD and TW, are likely to provide better spatial and temporal coverage. Understanding the relationship between the diurnal cycles of TD and TW, physiological thresholds and epidemiological dose-response curves also provides a promising avenue for future research.

In conclusion, we advocate for a more mechanistic understanding of both the diurnal cycles of TD and TW and the impacts of heat on human physiology^{12,42} as the way forward for designing climate adaptation strategies to heat in a warming climate.

Data and methods

Our analysis is restricted to the months of March–June since this is the heatwave season in South Asia (see Fig. 1). For reasons discussed in subsequent sections, we choose to select heatwave days based only on TD and not TW. We define regular days as those when the daily maximum TD lies between the 47.5th and 52.5th percentiles (i.e. close to the median value) and extreme days (i.e. heatwave days) as those when the daily maximum TD exceeds the 95th percentile. This calculation was done separately for each station and each of the four months.

Data. Station-level surface data from the Hadley Centre Integrated Surface Database (HadISD version 3.1.1.202006p;⁴³) was used to obtain temperature, relative humidity and surface pressure data for stations in South Asia. HadISD is a quality controlled sub daily dataset for various surface meteorological variables from 1950 till present. All stations from South Asia (Bangladesh, India and Pakistan) which had at least 6 hourly data for the time period 1995 until 2020 were selected (i.e. at least 12,200 observations). This selected 77 stations across South Asia, of which 55 stations had in excess of 20,000 observations, indicating nearly 3 hourly resolution for the entire duration of the analysis. For all stations, all available data was used which implies that there could be an underestimation of instances of high TD/TW in stations with lesser observations. Air temperature, dew point temperature and station level pressure were extracted and wet-bulb temperature was computed by solving the full nonlinear equation for adiabatic saturation temperature without any approximations²¹.

The Integrated Global Radiosonde Archive^{44,45} dataset was used to estimate boundary layer height and water vapour. Boundary layer height was estimated as the height of the top of inversion in the presence of surface-based inversions, and using the Parcel Method (based on Virtual Potential Temperature) for other instances⁴⁶. Where surface readings were absent, the next available reading was used if present within 500m of the surface. The mass of water vapour contained in the boundary layer was calculated as a mass-weighted integral of specific humidity over the entire boundary layer. Soundings which did not include valid values of dewpoint or air temperature below 500 hPa were discarded. Then, stations with greater than 65% available data over the time period of interest were filtered and days with multiple valid soundings were retained. The last filter of multiple soundings per day was applied so that at least one of the soundings would be close to the time of daily max TD. For analysing the timing of the diurnal cycle of TW, all the above filters except for the last one were applied for selecting stations.

Out of a total of 113 South Asian (Bangladesh, India and Pakistan) Integrated Global Radiosonde Archive stations, 72 were mapped to HadISD stations based on a maximum distance of 30 kilometres. Out of these, 37 stations met the data availability criteria above, for the time period 1995 until 2020. For these stations, only the vertical soundings that were available at within

an hour of the corresponding surface measurements were retained. This resulted in 10 station mappings with at least 6 hourly data. Some of these mappings made available data at 3 hourly resolution. Such data was used at the original time resolution and not subsampled. During one or more of the premonsoon months, all 10 of these stations saw a reduction in near-surface TW during times of extreme daily max TD. During other months, 5 of these stations saw a very small reduction in near-surface TW. Accordingly, 10 and 5 stations were used for evaluating boundary layer property changes under strong and weak amplifications of the diurnal cycle, respectively.

Health Impacts. Identification of high impact heatwaves was done using mortality data recorded during heatwaves in the Emergency Events Database (EM-DAT)⁴⁷ and corroborating press reports (see supplementary table S1). EM-DAT provides information about the country, regions affected and location (where available) of natural and technological disasters. For each such disaster, the type of disaster, mortality numbers as well as the start and end date is listed. EM-DAT is a country-level database, and therefore mortality is not spatially disaggregated by region for each disaster, but each country has a separate entry. For more details about EM-DAT, we refer the reader to <https://www.emdat.be/guidelines>. To obtain large-scale spatial patterns of mortality, annual mortality during heat waves for India was retrieved from the Open Government Data India portal⁴⁸ and the National Crime Records Bureau⁴⁹. The data was available for 2001–2018 across India which was then used for comparison between patterns of critical TW exceedance and mortality.

Meteorological conditions during high impact heat waves. We selected heatwaves that reported high mortality (more than a thousand recorded deaths) since 1995 using the EM-DAT database. This threshold selects for heatwaves that occurred in 1998, 2002, 2003 and 2015.

To study the meteorological conditions during these high-impact events, we chose to analyse data from stations located in regions that were severely affected. Andhra Pradesh is a region in India that was affected in all of these heatwaves based on the EM-DAT database as well as newspaper reports (supplementary table S1). The city of Karachi in Pakistan exceeded a thousand deaths in June 2015 and suffered a less severe heatwave in 2018. Based on this selection procedure, we chose to analyse station data from Karachi in Pakistan and a few stations from coastal Andhra Pradesh (see supplementary fig. S2 for the stations used) in India.

We note that our subsequent analysis of the diurnal cycle of TW includes all extreme days between 1995–2020 and not just these high impact events. We will show in subsequent sections that the TD/TW variability exhibited during these heatwaves is representative of the variability observed in many other stations in South Asia.

Diurnal cycle of TW. We attempt to understand the diurnal cycle of TW by looking at the variability of daily maximum and minimum TW separately.

To study the climatological relationship between the mean and standard deviation of TW, we bin stations based on their monthly mean TW using intervals of 5 degrees Celsius. Since our analysis includes 4 months, each station contributes four values to this analysis based on each month's mean TW. We then compute the standard deviation of daily maximum and minimum TW for each station for each bin to obtain a distribution of the standard deviation of TW across all stations in South Asia conditioned on the monthly mean TW.

Table 1 TD and TW values associated with uncompensable heat stress in thermal physiological experiments^{23,52}.

TD	36 °C	38 °C	40 °C	44.04 °C	47.48 °C	50.57 °C
TW	30.34 °C	30.96 °C	30.45 °C	27.82 °C	27.12 °C	25.75 °C

To study the change in daily maximum and minimum TW during heatwaves, the median value of daily maximum (**median(TW_{max})**) and minimum TW (**median(TW_{min})**) was computed for both regular and extreme days for each month. The diurnal range for regular and extreme days was computed as the difference between the median values of daily maximum and daily minimum values during regular and extreme days respectively (**Diurnal range = median(TW_{max}) – median(TW_{min})**). Our conclusions do not change if we use the median of the difference between the daily maximum and minimum TW instead (i.e., **median(TW_{max} – TW_{min})**). For each station and for each month, we define the change in the daily maximum, daily minimum and diurnal range of TW as the difference between the respective median values during regular and extreme days (for example, **change(TW_{max}) = median(TW_{max}) during extreme days – median(TW_{max}) during regular days**). By construction, the change in the diurnal range is equal to the sum of the change in the median daily maximum TW and median daily minimum TW. This definition implies that if the change in diurnal range is equal to change in daily minimum TW, the entire change in diurnal range is explained by the change in daily minimum TW, with the daily maximum TW remaining relatively unchanged.

To study the changes in boundary layer properties, we compute boundary layer (BL) heights and water vapour content as described previously for regular and extreme days. We then compute the mean and standard deviation of the BL heights and water vapour content and use these to normalise the individual observations by subtracting the mean and dividing by the standard deviation.

Critical TW exceedance in South Asia. In order to estimate likely health impacts, we used results from a thermal physiological study²³ which looked at the relationship between ambient wet and dry bulb temperatures and uncompensable heat stress – they used a heat chamber to directly measure the ambient TD and TW at which young, healthy, adult subjects experience uncompensable heat stress. We use their experimentally determined critical TW thresholds along with station data to calculate the number of instances when the combination of TD and TW were likely harmful to human health. For completeness, the threshold values from six different experiments reported in the above study are reproduced in Table 1. Since the lowest TD for which critical TW is available is 36 °C, we only consider instances with TD > 36 °C for our analysis. For TD > 50.57 °C the critical TW is taken to be constant at 25.75 °C, but since these values of TD are rarely reached, they are unlikely to change the overall picture presented subsequently.

These experiments were conducted in North America, and how these thresholds might change for an acclimatised South Asian population is unclear – they may be higher under similar conditions. Taking into account the effects of heat acclimation/acclimatisation is important especially in the context of the current study since it has been shown that the impacts of heat acclimation are most evident when experiencing conditions of uncompensable heat stress⁵⁰. However, it must be kept in mind that seasonal heat acclimatisation is a passive process and the magnitude of physiological adaptations that occur during this process are influenced by severity of the ambient thermal environment, timing and duration of environmental exposures

as well as duration and intensity of outdoor physical activity⁵¹. Additionally, there are other reasons to suggest that lower values of TW may also be harmful:

- The experiments were conducted indoors, and the absorption of shortwave and longwave radiation is likely to increase the total heat exposure.
- The volunteers in the experiments were young healthy adults, and it is known that the risk of mortality in older persons and those with co-morbidities such as cardiovascular disease and respiratory illnesses are higher⁴.
- The experimental protocol required study participants to be optimally hydrated before starting the experiment^{52,53}. In contrast, A recent survey of labourers in India showed that dehydration was common among the working population³¹. Cardiovascular function is impaired when dehydration is coupled with exposure to high temperatures⁵⁴, and heat exhaustion sets in at lower absolute core temperatures (and for smaller changes in core temperature) in heat acclimatised individuals who are dehydrated⁵⁵. Furthermore, it has been suggested that hypohydration negates the thermoregulation advantages conferred by heat acclimatisation⁵⁶.

Given these considerations, we not only look for absolute exceedances, but also exceedances of 0.95, 0.9 and 0.8 times the experimentally determined values. For every pair of TD and TW, we first compute the critical TW for the observed TD by linearly interpolating between the nearest two TD values from the experimental data. We then compare the critical TW (and its scaled versions) with the observed TW to compute the exceedances presented subsequently.

Data availability

The climate data used in this manuscript are available from the HadISD database (<https://www.metoffice.gov.uk/hadobs/hadisd/>), IGRA database (<https://www.ncei.noaa.gov/access/metadata/landing-page/bin/iso?id=gov.noaa.ncdc:C00975>) and ERA5 database (<https://cds.climate.copernicus.eu/cdsapp#!/dataset/reanalysis-era5-single-levels>). Mortality data attributed to heatwaves for India was obtained from the Open Government Data Portal (<https://data.gov.in/>) and the National Crime Records Bureau (<https://ncrb.gov.in/>), while aggregated mortality by country for South Asia is available from the EM-DAT database (<https://www.emdat.be/>). The links to individual press reports is provided in the supplementary material.

Code availability

For data processing and generating figures, we have used the Python libraries `xarray`⁵⁷, `matplotlib`⁵⁸, `pandas`⁵⁹, `cartopy` and `numpy`⁶⁰.

Received: 5 December 2022; Accepted: 16 June 2023;
Published online: 06 July 2023

References

1. Kovats, R. S. & Hajat, S. Heat stress and public health: a critical review. *Annu. Rev. Public Health* **29**, 41–55 (2008).
2. Green, H. et al. Impact of heat on mortality and morbidity in low and middle income countries: a review of the epidemiological evidence and considerations for future research. *Environ. Res.* **171**, 80–91 (2019).
3. Romanello, M. et al. The 2021 report of the Lancet Countdown on health and climate change: code red for a healthy future. *The Lancet* [https://doi.org/10.1016/S0140-6736\(21\)01787-6](https://doi.org/10.1016/S0140-6736(21)01787-6) (2021).

4. Ebi, K. L. et al. Hot weather and heat extremes: health risks. *The Lancet* **398**, 698–708 (2021).
5. Epstein, Y. & Moran, D. S. Thermal comfort and the heat stress indices. *Ind. Health* **44**, 388–398 (2006).
6. Jendritzky, G., de Dear, R. & Havenith, G. UTCI—Why another thermal index? *Int. J. Biometeorol.* **56**, 421–428 (2012).
7. Kampmann, B., Bröde, P. & Fiala, D. Physiological responses to temperature and humidity compared to the assessment by UTCI, WGBT and PHS. *Int. J. Biometeorol.* **56**, 505–513 (2012).
8. Bröde, P., Krüger, E. L., Rossi, F. A. & Fiala, D. Predicting urban outdoor thermal comfort by the Universal Thermal Climate Index UTCI—a case study in Southern Brazil. *Int. J. Biometeorol.* **56**, 471–480 (2012).
9. Blazejczyk, K., Epstein, Y., Jendritzky, G., Staiger, H. & Tinz, B. Comparison of UTCI to selected thermal indices. *Int. J. Biometeorol.* **56**, 515–535 (2012).
10. Buzan, J. R., Oleson, K. & Huber, M. Implementation and comparison of a suite of heat stress metrics within the Community Land Model version 4.5. *Geosci. Model Dev.* **8**, 151–170 (2015).
11. Buzan, J. R. & Huber, M. Moist heat stress on a hotter Earth. *Annu. Rev. Earth Planet. Sci.* **48**, 623–655 (2020).
12. Vanos, J. K., Baldwin, J. W., Jay, O. & Ebi, K. L. Simplicity lacks robustness when projecting heat-health outcomes in a changing climate. *Nat. Commun.* **11**, 6079 (2020).
13. Cramer, M. N. & Jay, O. Biophysical aspects of human thermoregulation during heat stress. *Auton. Neurosci.* **196**, 3–13 (2016).
14. Sherwood, S. C. & Huber, M. An adaptability limit to climate change due to heat stress. *Proc. Natl Acad. Sci. USA* **107**, 9552–9555 (2010).
15. Im, E.-S., Pal, J. S. & Eltahir, E. A. B. Deadly heat waves projected in the densely populated agricultural regions of South Asia. *Sci. Adv.* **3**, e1603322 (2017).
16. Mishra, V., Mukherjee, S., Kumar, R. & Stone, D. A. Heat wave exposure in India in current, 1.5 °C, and 2.0 °C worlds. *Environ. Res. Lett.* **12**, 124012 (2017).
17. Raymond, C., Matthews, T. & Horton, R. M. The emergence of heat and humidity too severe for human tolerance. *Sci. Adv.* **6**, eaaw1838 (2020).
18. Romanello, M. et al. The 2021 report of the Lancet Countdown on health and climate change: code red for a healthy future. *The Lancet* **398**, 1619–1662 (2021).
19. Pai, D. S., Nair, S. A. & Ramanathan, A. N. Long term climatology and trends of heat waves over India during the recent 50 years (1961–2010). *Mausam* **20**, 585–604 (2013).
20. Ratnam, J. V., Behera, S. K., Ratna, S. B., Rajeevan, M. & Yamagata, T. Anatomy of Indian heatwaves. *Sci. Rep.* **6**, 24395 (2016).
21. Monteiro, J. M. & Caballero, R. Characterization of extreme wet-bulb temperature events in Southern Pakistan. *Geophys. Res. Lett.* **46**, 10659–10668 (2019).
22. Rogers, C. D. W. et al. Recent increases in exposure to extreme humid-heat events disproportionately affect populated regions. *Geophys. Res. Lett.* **48**, e2021GL094183 (2021).
23. Vecellio, D. J., Wolf, S. T., Cottle, R. M. & Kenney, W. L. Evaluating the 35°C wet-bulb temperature adaptability threshold for young, healthy subjects (PSU HEAT Project). *J. Appl. Physiol.* **132**, 340–345 (2022).
24. Azhar, G. S. et al. Heat-related mortality in India: excess all-cause mortality associated with the 2010 Ahmedabad heat wave. *PLoS ONE* **9**, e91831 (2014).
25. Mazdiyasni, O. et al. Increasing probability of mortality during Indian heat waves. *Sci. Adv.* **3**, e1700066 (2017).
26. Nori-Sarma, A. et al. The impact of heat waves on mortality in Northwest India. *Environ. Res.* **176**, 108546 (2019).
27. Dimitrova, A. et al. Association between ambient temperature and heat waves with mortality in South Asia: systematic review and meta-analysis. *Environ. Int.* **146**, 106170 (2021).
28. Ingole, V., Sheridan, S. C., Juvekar, S., Achebak, H. & Moraga, P. Mortality risk attributable to high and low ambient temperature in Pune city, India: a time series analysis from 2004 to 2012. *Environ. Res.* <https://www.sciencedirect.com/science/article/pii/S0013935121016054> (2021).
29. Janowiak, J. E. & Xie, P. A global-scale examination of monsoon-related precipitation. *J. Clim.* **16**, 4121–4133 (2003).
30. Wehner, M., Stone, D., Krishnan, H., AchutaRao, K. & Castillo, F. The deadly combination of heat and humidity in India and Pakistan in summer 2015. *Bull. Am. Meteorol. Soc.* **97**, S81–S86 (2016).
31. Venugopal, V. et al. Epidemiological evidence from south Indian working population-the heat exposures and health linkage. *J. Exp. Sci. Environ. Epidemiol.* **31**, 177–186 (2021).
32. Jiang, S., Lee, X., Wang, J. & Wang, K. Amplified urban heat islands during heat wave periods. *J. Geophys. Res. Atmos.* **124**, 7797–7812 (2019).
33. Nicholson, A. Analysis of the diurnal cycle of air temperature between rural Berkshire and the University of Reading: possible role of the urban heat island. *Weather* **75**, 235–241 (2020).
34. Wang, P., Li, D., Liao, W., Rigden, A. & Wang, W. Contrasting evaporative responses of ecosystems to heatwaves traced to the opposing roles of vapor pressure deficit and surface resistance. *Water Resour. Res.* **55**, 4550–4563 (2019).
35. Jay, O. et al. Reducing the health effects of hot weather and heat extremes: from personal cooling strategies to green cities. *The Lancet* **398**, 709–724 (2021).
36. Raymond, C. et al. On the controlling factors for globally extreme humid heat. *Geophys. Res. Lett.* <https://doi.org/10.1029/2021GL096082> (2021).
37. Zhang, Y. & Fueglistaler, S. How tropical convection couples high moist static energy over land and ocean. *Geophys. Res. Lett.* <http://agupubs.onlinelibrary.wiley.com/doi/abs/10.1029/2019GL086387> (2020).
38. Zhang, Y., Held, I. & Fueglistaler, S. Projections of tropical heat stress constrained by atmospheric dynamics. *Nat. Geosci.* **14**, 133–137 (2021).
39. Pörtner, H.-O. et al. *Climate Change 2022: Impacts, Adaptation and Vulnerability* (IPCC Geneva, 2022).
40. Baldwin, J. W. et al. Humidity's role in heat-related health outcomes: a heated debate. *Environ. Health Perspect.* **131**, 055001 (2023).
41. Municipal Corporation, A. *Ahmedabad Heat Action Plan – Easy Read Version* (2019).
42. Kenney, W. L., Havenith, G. & Jay, O. Thermal physiology, more relevant than ever before. *J. Appl. Physiol.* **133**, 676–678 (2022).
43. Dunn, R. Hadisid version 3: Monthly updates. hadley centre tech. *Tech. Rep. Note* 103, 10 (2019).
44. Durre, I., Yin, X., Vose, R. S., Applequist, S. & Arnfield, J. Enhancing the data coverage in the integrated global radiosonde archive. *J. Atmos. Ocean. Technol.* **35**, 1753–1770 (2018).
45. Durre, I., Vose, R. S. & Wuertz, D. B. Overview of the integrated global radiosonde archive. *J. Clim.* **19**, 53–68 (2006).
46. Seidel, D. J., Ao, C. O. & Li, K. Estimating climatological planetary boundary layer heights from radiosonde observations: Comparison of methods and uncertainty analysis. *J. Geophys. Res.* **115**, D16113 (2010).
47. EM-DAT. EM-DAT, CRED / UCLouvain, Brussels, Belgium. www.emdat.be (2022).
48. OGD. *Open Government Data (OGD) platform*. <https://data.gov.in> (2021).
49. NCRB. *National Crime Records Bureau*. <https://ncrb.gov.in/> (2021).
50. Ravanelli, N., Coombs, G., Imbeault, P. & Jay, O. Thermoregulatory adaptations with progressive heat acclimation are predominantly evident in uncompensable, but not compensable, conditions. *J. Appl. Physiol.* **127**, 1095–1106 (2019).
51. Brown, H. A. et al. Seasonal heat acclimatisation in healthy adults: a systematic review. *Sports Med.* **52**, 2111–2128 (2022).
52. Wolf, S. T., Cottle, R. M., Vecellio, D. J. & Kenney, W. L. Critical environmental limits for young, healthy adults (PSU HEAT Project). *J. Appl. Physiol.* **132**, 327–333 (2022).
53. Cottle, R. M., Wolf, S. T., Lichter, Z. S. & Kenney, W. L. Validity and reliability of a protocol to establish human critical environmental limits (PSU HEAT Project). *J. Appl. Physiol.* **132**, 334–339 (2022).
54. José, G.-A., Mora-Rodríguez, R., Below, P. R. & Coyle, E. F. Dehydration markedly impairs cardiovascular function in hyperthermic endurance athletes during exercise. *J. Appl. Physiol.* **82**, 1229–1236 (1997).
55. Sawka, M. N. et al. Human tolerance to heat strain during exercise: influence of hydration. *J. Appl. Physiol.* **73**, 368–375 (1992).
56. Sawka, M. N., Montain, S. J. & Latzka, W. A. Hydration effects on thermoregulation and performance in the heat. *Comp. Biochem. Physiol. Part A Mol. Integr. Physiol.* **128**, 679–690 (2001).
57. Hoyer, S. & Hamman, J. xarray: Nd labeled arrays and datasets in python. *J. Open Res. Softw.* **5**, 10 (2017).
58. Hunter, J. D. Matplotlib: A 2d graphics environment. *Comput. Sci. Eng.* **9**, 90–95 (2007).
59. McKinney, W. et al. pandas: a foundational python library for data analysis and statistics. *Python For High Performance And Scientific Computing*. **14**, 1–9 (2011).
60. Harris, C. R. et al. Array programming with numpy. *Nature* **585**, 357–362 (2020).

Acknowledgements

J.M.M. and J.J. were partly funded by the Science and Engineering Board (SERB) Startup Research Grant SRG/2020/000062. J.M.M. thanks Matthew Huber for useful discussions during the course of this project.

Author contributions

J.J. contributed to data processing and analysis, writing and reviewing the manuscript. J.M.M. contributed to research design, data processing and analysis, writing and reviewing the manuscript. H.S. contributed to data processing and analysis, writing and reviewing the manuscript. N.R. contributed to research design, writing and reviewing the manuscript.

Competing interests

J.M.M. is an Editorial Board Member for Communications Earth and Environment, but was not involved in the editorial review of, nor the decision to publish this article. All other authors declare no competing interests.

Additional information

Supplementary information The online version contains supplementary material available at <https://doi.org/10.1038/s43247-023-00897-0>.

Correspondence and requests for materials should be addressed to Joy Merwin Monteiro.

Peer review information *Communications Earth & Environment* thanks Ana Oliveira and the other, anonymous, reviewer(s) for their contribution to the peer review of this work. Primary Handling Editors: Heike Langenberg. A peer review file is available

Reprints and permission information is available at <http://www.nature.com/reprints>

Publisher's note Springer Nature remains neutral with regard to jurisdictional claims in published maps and institutional affiliations.



Open Access This article is licensed under a Creative Commons Attribution 4.0 International License, which permits use, sharing, adaptation, distribution and reproduction in any medium or format, as long as you give appropriate credit to the original author(s) and the source, provide a link to the Creative Commons license, and indicate if changes were made. The images or other third party material in this article are included in the article's Creative Commons license, unless indicated otherwise in a credit line to the material. If material is not included in the article's Creative Commons license and your intended use is not permitted by statutory regulation or exceeds the permitted use, you will need to obtain permission directly from the copyright holder. To view a copy of this license, visit <http://creativecommons.org/licenses/by/4.0/>.

© The Author(s) 2023, corrected publication 2023